

1 **Supporting Information**

2

3 **Temperature-Programmed Reduction Method for Stabilization of**
4 **Inorganic Framework of SAPO-37 Materials: Promising Catalysts**
5 **for MTBE Production**

6

7 **K. Khadheejath Shabana,^a Soumya B. Narendranath,^a N. P. Nimisha,^a N. J. Venkatesha,^b**
8 **G. Sheetal,^c and A. Sakthivel^{a*}**

9

10 *^[a]Inorganic Materials & Heterogeneous Catalysis Laboratory, Department of Chemistry,*
11 *School of Physical Sciences, Sabarmati Building, Tejaswini Hills,*
12 *Central University of Kerala, Kasaragod - 671320, India.*

13 **Email: sakthiveldu@gmail.com / sakthivelcuk@cukerala.ac.in*

14 *ORCID information: <https://orcid.org/0000-0003-2330-5192>*

15 *<https://orcid.org/0000-0002-5483-6327>*

16 *^[b]Department of Chemistry, Bangalore Institute of Technology, Bangalore, 560004, India*

17 *^[c]Catalysis and Inorganic Chemistry Division,*
18 *CSIR-National Chemical Laboratory, Pune, India*

19

20

21

22 **Experimental**

23 **Materials & Synthesis Protocol:**

24 The following chemicals were used: pseudo boehmite (Al₂O₃, 75%, BeeChems, grade
25 PSB-M), ortho phosphoric acid (H₃PO₄, 85%, Merck), fumed silica (Aerosil 200,
26 Aldrich), tetra propyl ammonium hydroxide (TPAOH, 40% aqueous solution), tetra
27 methyl ammonium hydroxide (TMAOH, 25% aqueous solution, TriTech Catalyst and
28 Intermediate), ammonium heptamolybdate tetra hydrate ((NH₄)₆Mo₇O₂₄·4H₂O, SRL), D-
29 glucose (Fischer Scientific), methanol and *tert*-butyl alcohol (extra pure AR, SRL).

1 The SAPO-37 samples were synthesized using a hydrothermal method following a
2 previously reported procedure.^{7,12} The molar gel composition was $(\text{TPA})_2\text{O}$:
3 $0.025(\text{TMA})_2\text{O}$: Al_2O_3 : P_2O_5 : 0.43SiO_2 : $50.0\text{H}_2\text{O}$. Solution I was prepared by slowly
4 adding pseudo boehmite to dilute orthophosphoric acid while stirring. Solution II was
5 prepared by adding fumed silica to a mixture of TPAOH and TMAOH. The final gel was
6 obtained by adding Solution II to Solution I while vigorously stirring. The resulting slurry
7 was packed in a stainless-steel autoclave with Teflon liners and heated at 200 °C under
8 autogenous pressure for 20 h. The product was then separated via centrifugation, washed
9 with deionized water, and dried at 60 °C. The obtained sample was labeled as SAP-37.
10 The as-prepared materials were dried in an air oven at 200 °C and subsequently reduced
11 under temperature programmed mode in a hydrogen atmosphere at 550 °C. The TPR-
12 treated sample is denoted as SAP-37R.

13 To stabilize SAPO-37 with improved activity, this study focused on the incorporation of
14 Mo species during the TPR process, generating an SAPO-37 framework containing Mo
15 carbide-type species. For the same, molybdenum blue type species was used, which was
16 prepared according to a reported procedure using ammonium heptamolybdate
17 tetrahydrate as the molybdenum source and D-glucose as the reducing agent (R). In this
18 regard, it is worth mention here that the pH of the reaction mixture defines the size of
19 molybdenum blue. The self-organization of molybdenum blue into gigantic wheel-shaped
20 clusters containing $\{\text{Mo}_{154}\}$ ¹¹ with a diameter of 3.4 nm usually takes place at low pH
21 ($\text{pH} < 2$) and at a low ratio of [reducing agent] to [molybdate]. Isopolymolybdate $\{\text{Mo}_{36}\}$
22 is formed at a pH of 1.7.¹¹ Here, we synthesized molybdenum blue at a pH of 2 and at a
23 higher ratio of [reducing agent] to [molybdate], which facilitates the formation of
24 molybdenum blue building blocks with a size of around 6 Å. These blocks can easily
25 enter the SAPO-37 cavities.

26 For the incorporation of molybdenum species and subsequent stabilization of the
27 framework via TPR, molybdenum blue with an R/Mo ratio of 4 was introduced (0.6 g of
28 molybdenum blue per gram) into the pore volume of as-prepared SAPO-37 and
29 subsequently dried at 80 °C for 12 h. This procedure was repeated thrice. For comparison,
30 Mo blue with different R/Mo ratios, including 2, 5, and 6, on SAPO-37 were prepared.
31 All the prepared samples were stabilized using the TPR method at 550 °C for 2 h. SAPO-

1 37 stabilized by the TPR method in the presence of molybdenum blue with different
2 R/Mo ratios (2, 4, 5, and 6), is denoted as SAP-37MoC-2R, SAP-37MoC-4R, SAP-
3 37MoC-5R, and SAP-37MoC-6R.

4 **Characterization Methods:**

5 Fourier transform infrared spectroscopy (FTIR) was conducted on the prepared catalysts
6 using a Jasco FT-IR spectrometer in the mid-IR region 4000–400 cm^{-1} via the ATR
7 method. Powder X-ray diffraction (XRD) analysis was performed using a PAN analytical
8 X'pert3 powder X-ray diffractometer with Cu $K\alpha$ radiation of 1.5405 Å, scanning in the
9 range of $2\theta = 5^\circ\text{--}80^\circ$.

10 Surface elemental analysis was conducted using X-ray photoelectron spectroscopy (XPS).
11 This analysis was performed using a photoelectron spectrometer (Pervac, Poland)
12 equipped with a VG Scienta R3000HP analyzer and an MX650 monochromator. XPS
13 spectra were deconvoluted to obtain various oxidation states using the Shirley method for
14 baseline correction. The peak fit conditions used were: full-width half maxima (FWHM):
15 1.3 ± 0.1 eV, $3d_{5/2}\text{--}3d_{3/2}$ distance 3.2 eV and the ratio of $3d_{5/2}/3d_{3/2}=3/2$.

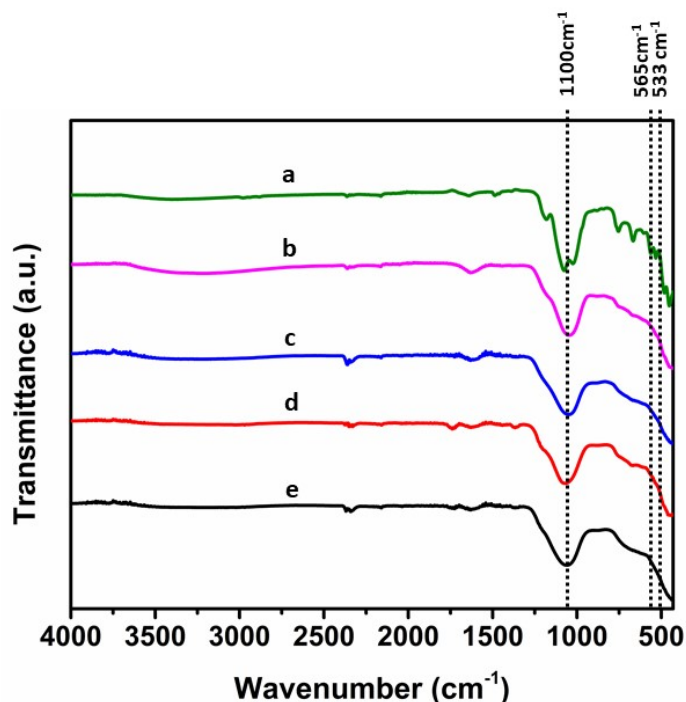
16 The organic contents of the as-synthesized SAPO-37 and molybdenum-stabilized SAPO-
17 37 were examined via thermogravimetric analysis (TGA) using a PerkinElmer STA 6000
18 simultaneous thermal analyzer. TGA was conducted in a nitrogen atmosphere within the
19 temperature range of 35 to 900 $^\circ\text{C}$ with a heating rate of 10 $^\circ\text{C}/\text{min}$. The morphologies of
20 the synthesized materials were analyzed using scanning electron microscopy (SEM,
21 TESCAN VEGA3) at 300 kV. TEM images were recorded using a transmission electron
22 microscope (M/s JOEL JEM 2100). Solid state NMR spectra were obtained on Bruker
23 Avance III HD at 9.4 T using zirconia rotors with spinning speed of 7 kHz.

24 The acidic properties of the prepared catalysts were examined via NH_3 -TPD using a
25 BELCAT-M instrument (Japan). The sample was preheated at 400 $^\circ\text{C}$ for 30 min in a
26 quartz reactor. Ammonia adsorption was conducted at 50 $^\circ\text{C}$ for 30 min, followed by
27 desorption at 50 $^\circ\text{C}$ to remove physisorbed ammonia. The measurements were performed
28 from 50 $^\circ\text{C}$ to 600 $^\circ\text{C}$ at a heating rate of 10 $^\circ\text{C}/\text{min}$. The quantification of Brønsted and
29 Lewis acid sites was studied by pyridine FTIR analysis performed on a NICOLET iS50
30 spectrometer in the range of 4000-400 cm^{-1} using an MCTB detector. The textural
31 properties, such as BET surface area and pore volume, were determined through nitrogen

1 sorption analysis using an automatic micropore physisorption analyzer (Quanta Chrome
2 Nova 10-7) at $-196\text{ }^{\circ}\text{C}$. Prior to sorption measurements, samples were degassed at $110\text{ }^{\circ}\text{C}$
3 under a pressure of 10^{-3} Torr. The chemical composition of samples was followed by
4 inductively coupled plasma atomic emission spectroscopy (ICP-AES) using the MP-AES
5 instrument.

6 **Catalytic Studies:**

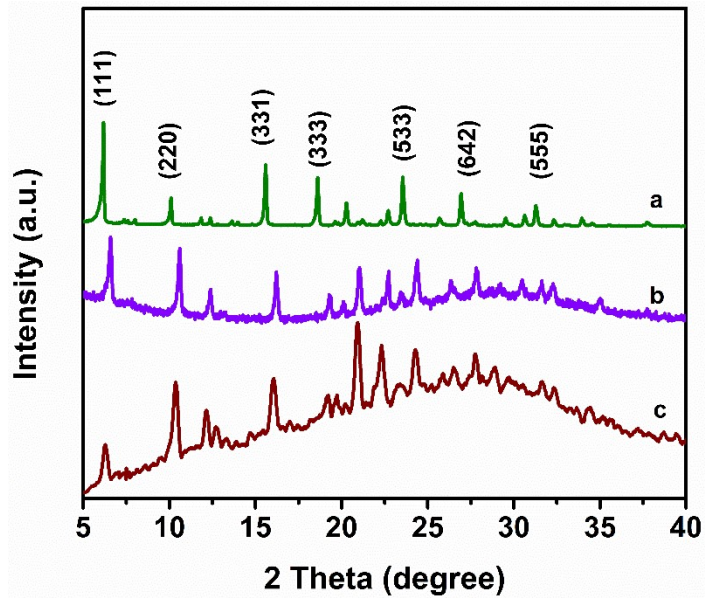
7 The prepared catalyst was investigated for the synthesis of MTBE from methyl alcohol
8 and tertiary-butyl alcohol (TBA) in a 100 mL stainless autoclave. In a typical reaction,
9 0.05 g of catalyst was mixed with 30 mmol of methyl alcohol and 10 mmol of TBA. The
10 reaction conditions were optimized with different temperatures ($120\text{--}160\text{ }^{\circ}\text{C}$) and
11 durations of 2 to 8 h. After the reaction, the products and catalysts were separated via
12 centrifugation. The products were confirmed using authentic samples and analyzed using
13 gas chromatography (Mayura Analytical model 1100) with a flame ionization detector
14 equipped with an HP-5 capillary column (30 m (length) x 0.25 mm (inner diameter), $0.25\text{ }\mu\text{m}$
15 (film thickness)). The temperature program mode used was heating from $60\text{ to }70\text{ }^{\circ}\text{C}$
16 ($1\text{ }^{\circ}\text{C}/\text{min}$) and then from $70\text{ to }240\text{ }^{\circ}\text{C}$ ($10\text{ }^{\circ}\text{C}/\text{min}$).



17

18 Fig. S1. FTIR spectra of a) SAP-37as, b) SAP-37MoC-6R, c) SAP-37MoC-5R, d) SAP-37MoC-
19 4R, and e) SAP-37MoC-2R.

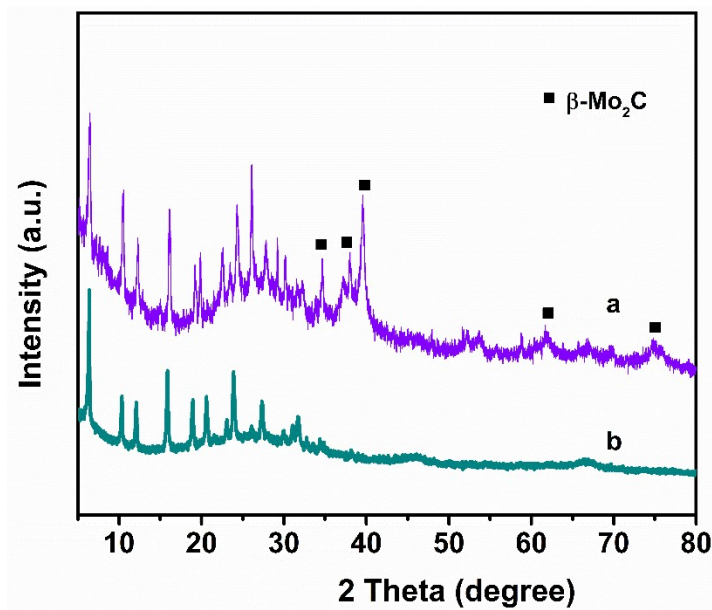
1



2

3 Fig. S2. Powder XRD of a) SAP-37as, b) SAP-37R, and c) used SAP-37R.

4



5

6 Fig. S3. Powder XRD of a) SAP-37MoC-4R', and b) SAP-37MoC-4R.

7

8

9

1

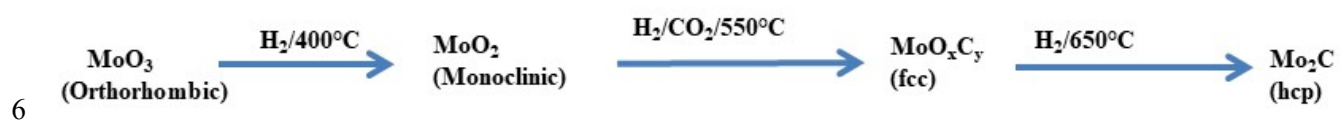
2 Table S1. Binding energy for various molybdenum and carbon species.

3

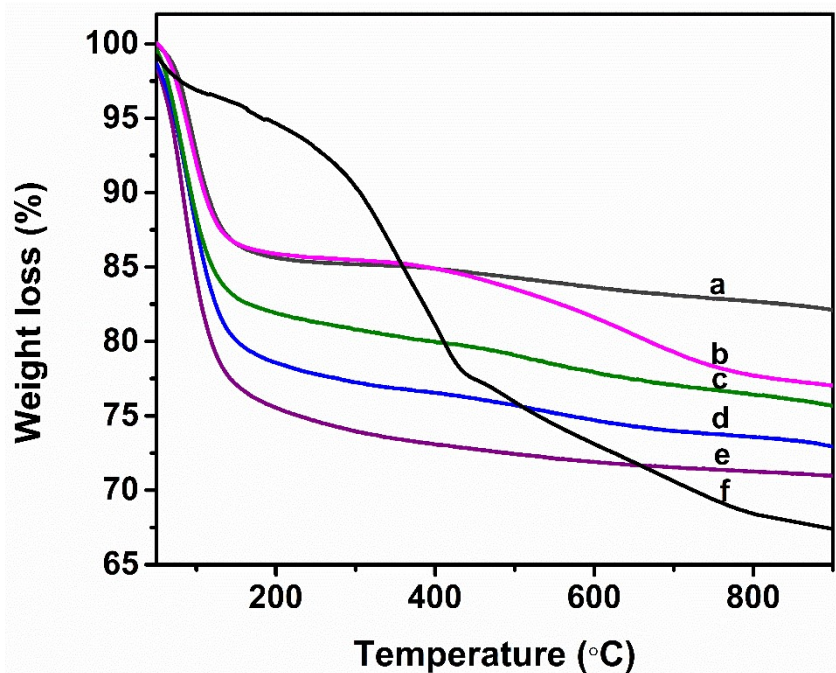
Mo species	Binding energy (eV)	
	3d _{5/2}	3d _{3/2}
Mo ⁶⁺	232.7	235.8
Mo ⁵⁺	231.7	235
Mo ⁴⁺	230.1	233.8
Mo ²⁺	228.8	232.1
C species	1s	
Csp ³	284.8	
C=O	288.6	
C-O	286.4	
C-O-Mo	283.9	

4

5



7 Scheme S1. Mechanism for molybdenum (oxy) carbide formation.



1

2 Fig. S4. TGA profile of a) SAP-37MoC-2R, b) SAP-37MoC-4R, c) SAP-37MoC-6R, d) SAP-
 3 37MoC-5R, e) SAP-37R, and f) SAP-37as.

4

5 Table S2. Thermogravimetric weight loss of TPR treated SAPO-37.

Sample	Weight loss (%)			Total (%)
	Below 200 °C	200-450 °C	Above 450 °C	
SAP-37 as	7	16	9	32
SAP-37R	24	3	1	28
SAP-37MoC-2R	14	2	2	18
SAP-37MoC-4R	14	2	7	23
SAP-37MoC-5R	20	3	3	26
SAP-37MoC-6R	18	3	4	25

6

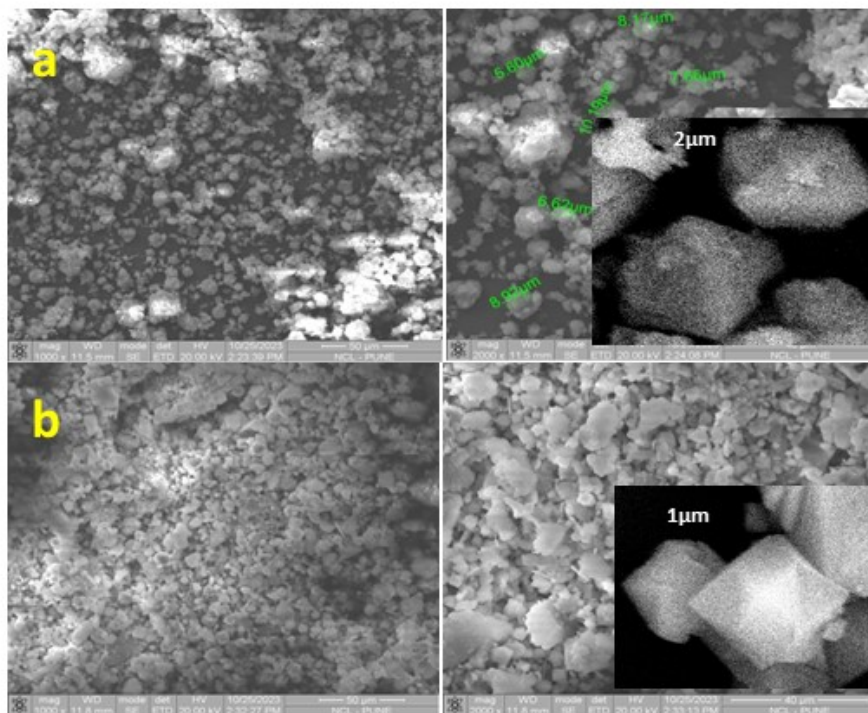
7

1

2 Scanning Electron Micrographs

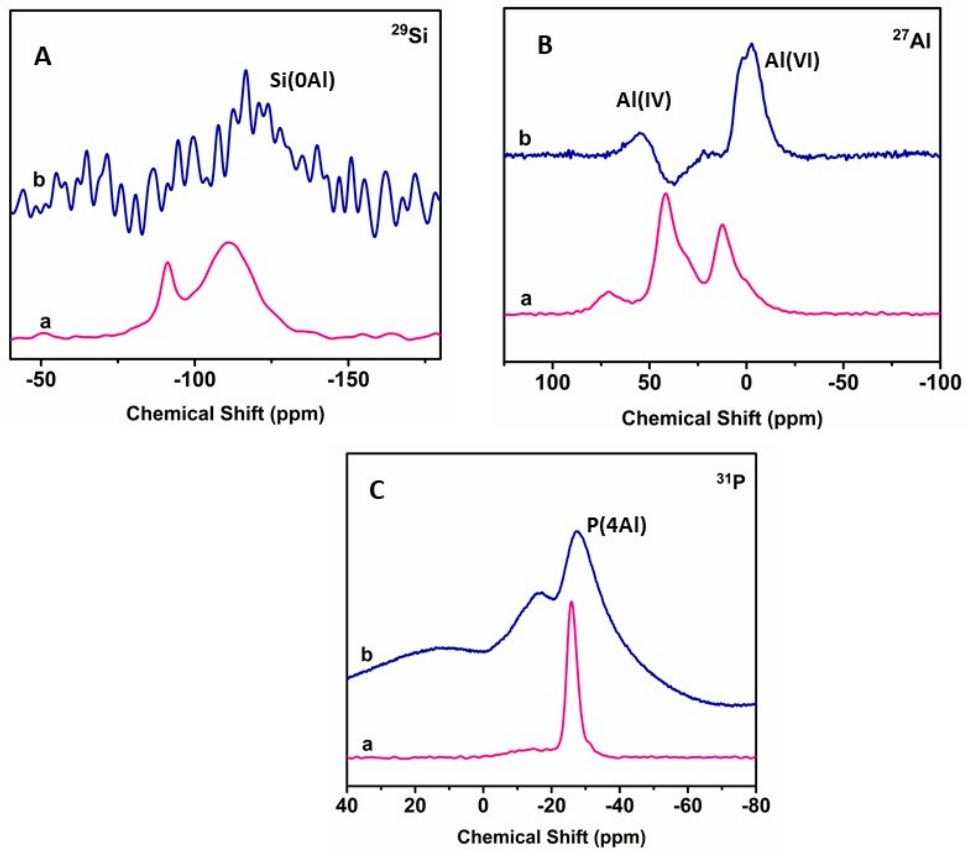
3 Morphological deterioration after template removal was confirmed from the SEM images. As
4 shown in Fig. S5 (ESI), SEM images of the as-prepared SAPO-37 and TPR-treated samples
5 (SAP-37MoC-4R) show a distorted cubic shape with good crystallinity.¹⁸ The SEM images
6 confirm that the TPR treatment and MoOC species in the framework helped to retain the
7 faujasite topology of SAPO-37, which is in good agreement with the XRD pattern. Moreover,
8 the incorporation of MoOC facilitated the homogeneous dispersion of the SAPO-37 particles.
9 The average particle size of the parent SAPO-37 is 2–7 μm , while that of molybdenum (oxy)
10 carbide incorporated SAPO-37 is 5-10 μm .

11



12

13 Fig. S5. Scanning Electron Micrographs of a) SAP-37MoC-4R, and b) SAP-37as.

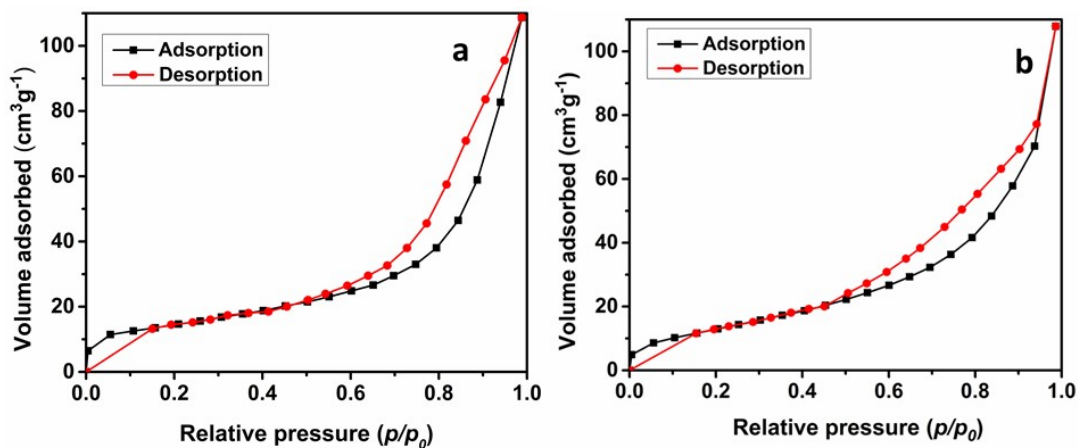


1

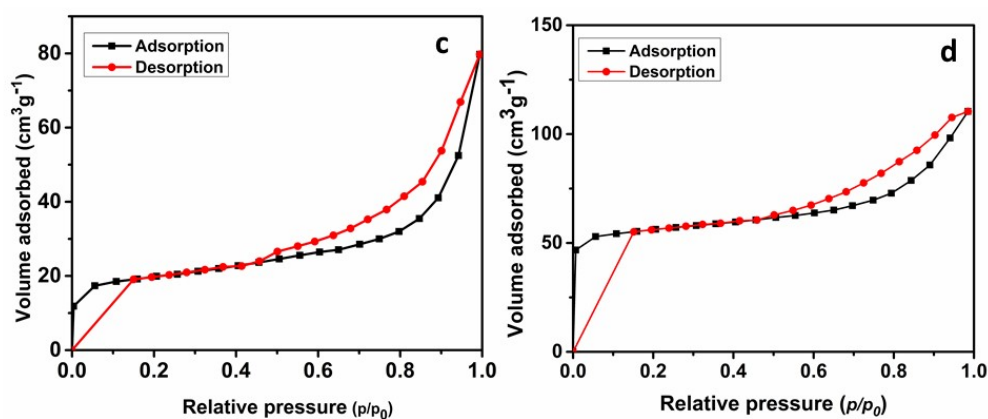
2 Fig. S6. ^{29}Si (A), ^{27}Al (B), and ^{31}P (C) MAS NMR spectra of a) SAP-37R, and b) SAP-37MoC-
 3 4R.

4

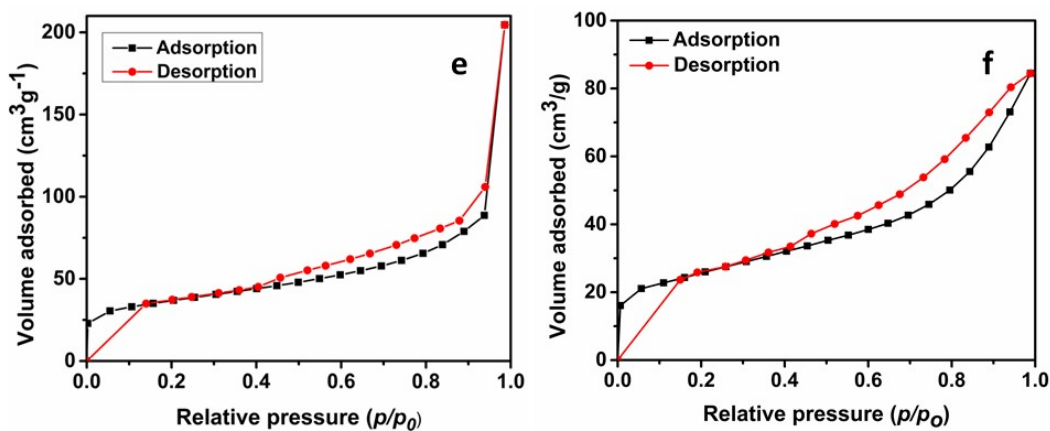
5



1



2



3

4

5 Fig. S7. N₂ sorption isotherm of TPR reduced SAPO-37 a) SAP-37R, b) SAP-37MoC-2R, c)
 6 SAP-37MoC-5R, d) SAP-37MoC-6R, e) SAP-37MoC-4R, and f) Used SAP-37MoC-4R.

7

1 Nitrogen sorption analysis (Fig. S7, ESI) shows Type-I isotherm with a sharp uptake in the p/p_0
 2 range of 0.1, which is characteristic of the microporous SAPO-37 framework. Moreover,
 3 additional isotherms show continuous adsorption in the higher p/p_0 range owing to interparticle
 4 mesoporosity. The low surface area of 128 m²/g can be attributed to the incorporation of
 5 molybdenum species into the faujasite structure. BET surface area and pore volume of TPR
 6 treated samples summarized in Table S4 (ESI). The introduction of molybdenum blue precursor
 7 and subsequent reduction increases the pore volume (SAP-37MoC-4R) due to the stabilization of
 8 the SAPO-37 framework and accessibility of channels and cavities. However, the increase in the
 9 R/Mo ratio facilitates carbon deposition and the reduction in the pore volume of SAP-37MoC-5R
 10 and SAP-37MoC-6R. SAP-37MoC-6R showed a high surface area due to the formation of
 11 porous carbon.

12

13

14 Table S3. Elemental composition of reduced SAPO-37 samples

Samples	Elemental composition (weight %)‡			
	Si	Al	P	Mo
SAP-37R	4.9	12.7	11.6	0
SAP-37MoC-2R	5.7	14.8	13.0	5.1
SAP-37MoC-4R	5.4	13.9	11.8	5.2
SAP-37MoC-6R	5.2	13.5	11.6	4.4

15

16

17

18

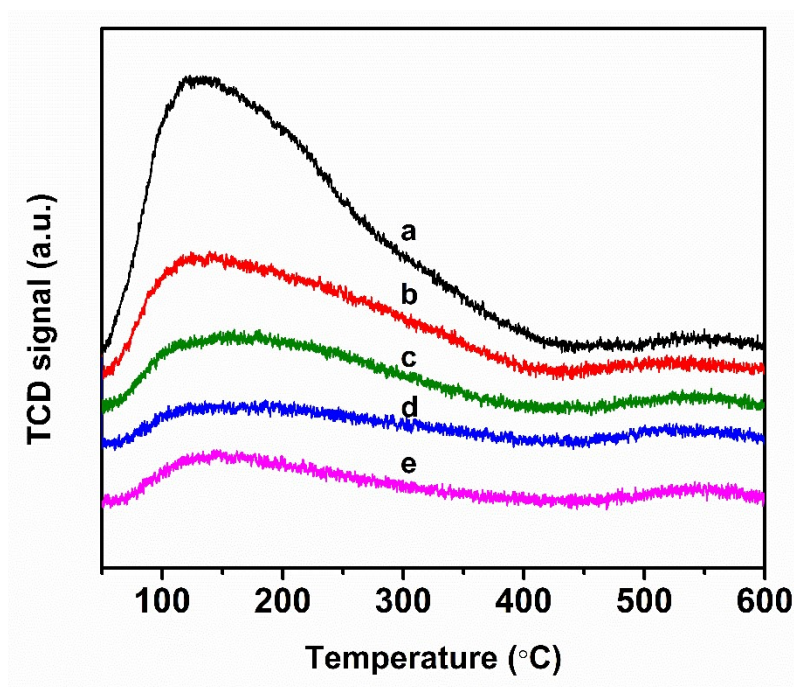
19

1 Table S4. BET surface area and pore volume of TPR treated samples

Samples	BET surface area (m ² /g)	Pore volume (cc/g)
SAP-37R	51	0.176
SAP-37MoC-2R	51	0.190
SAP-37MoC-4R	128	0.295
SAP-37MoC-5R	72	0.116
SAP-37MoC-6R	123	0.139

2

3



4

5 Fig. S8. NH₃ –TPD of a) SAP-37MoC-4R, b) SAP-37MoC-5R, c) SAP-37MoC-2R, d) SAP-
6 37MoC-6R, and e) SAP-37R.

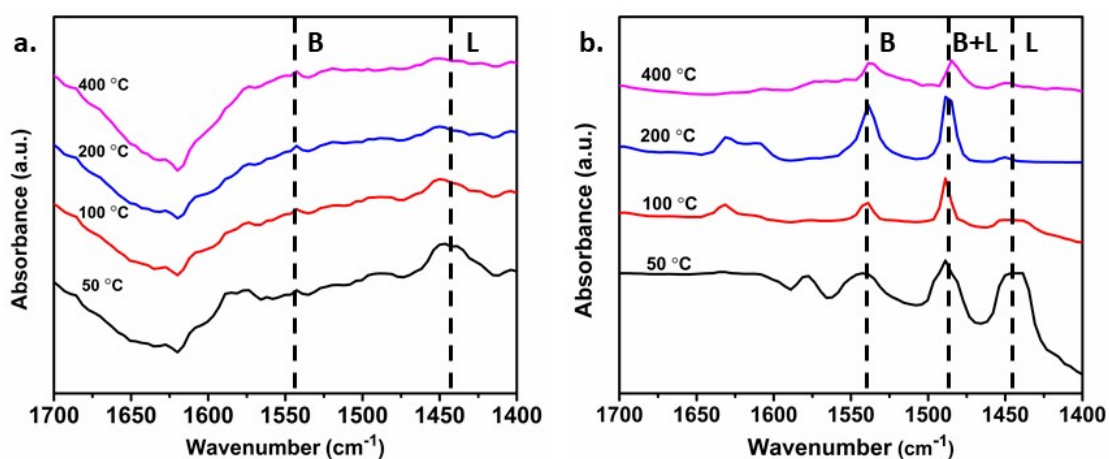
7

8

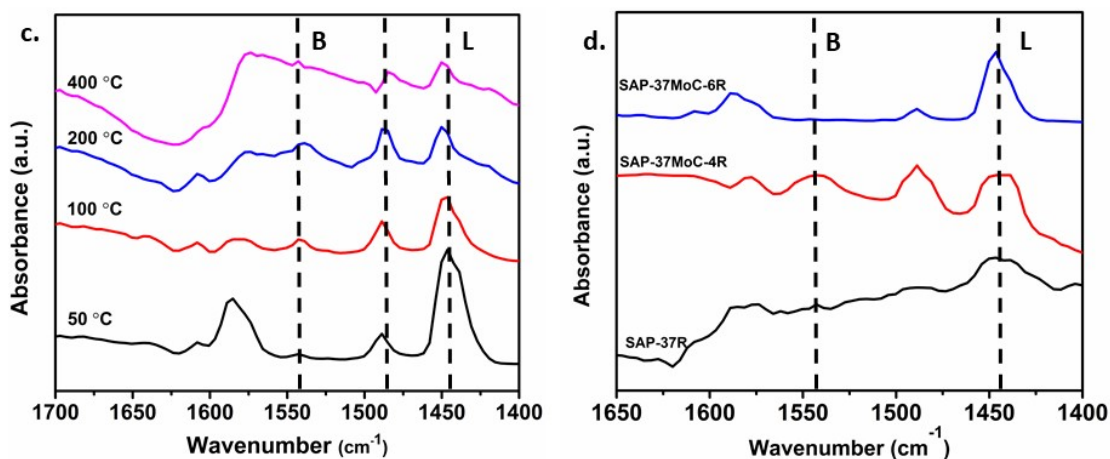
1 Table S5 Total amount of acid sites of TPR treated SAPO-37 samples.

Catalyst	Amount of ammonia desorbed (mmol/g)
SAP-37- R	0.125
SAP-37-MoC-2R	0.275
SAP-37-MoC-4R	0.700
SAP-37-MoC-5R	0.350
SAP-37-MoC-6R	0.125

2



3

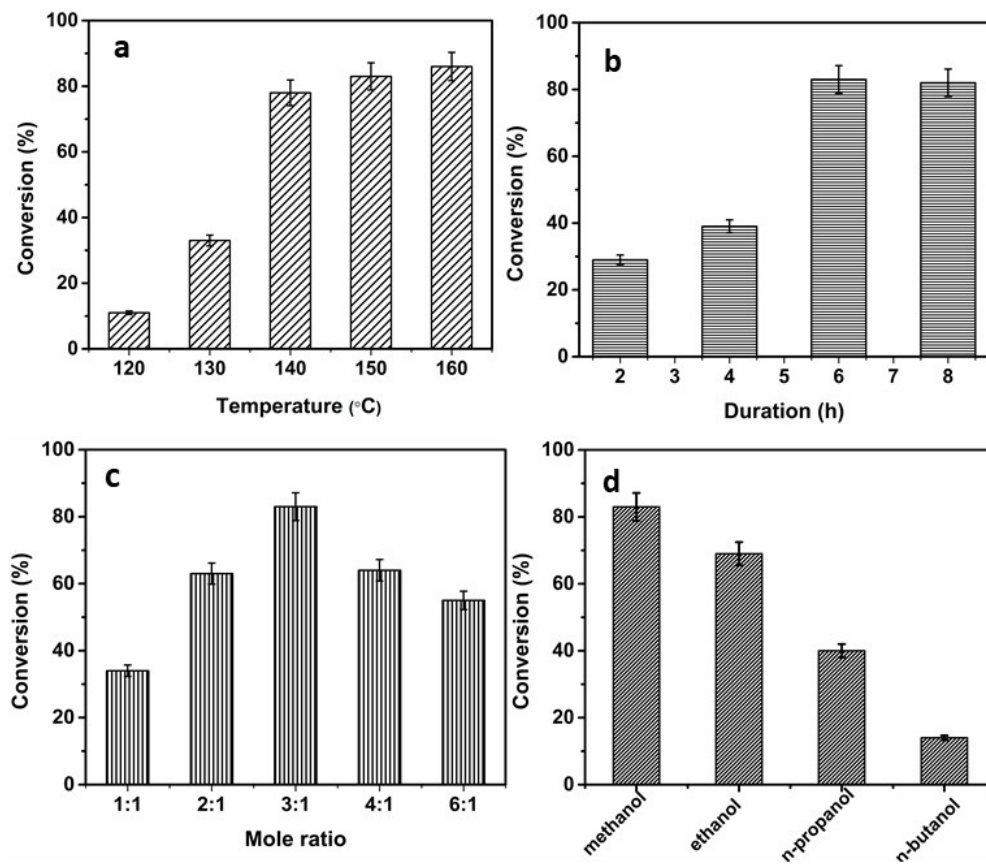


4

5 Fig. S9. The effect of molybdenum loading on pyridine-desorption FTIR spectra a) SAP-37R, b)
6 SAP-37MoC-4R, c) SAP-37MoC-6R, and d) pyridine-desorption spectra obtained at 50 °C for
7 various TPR treated samples.

1

2

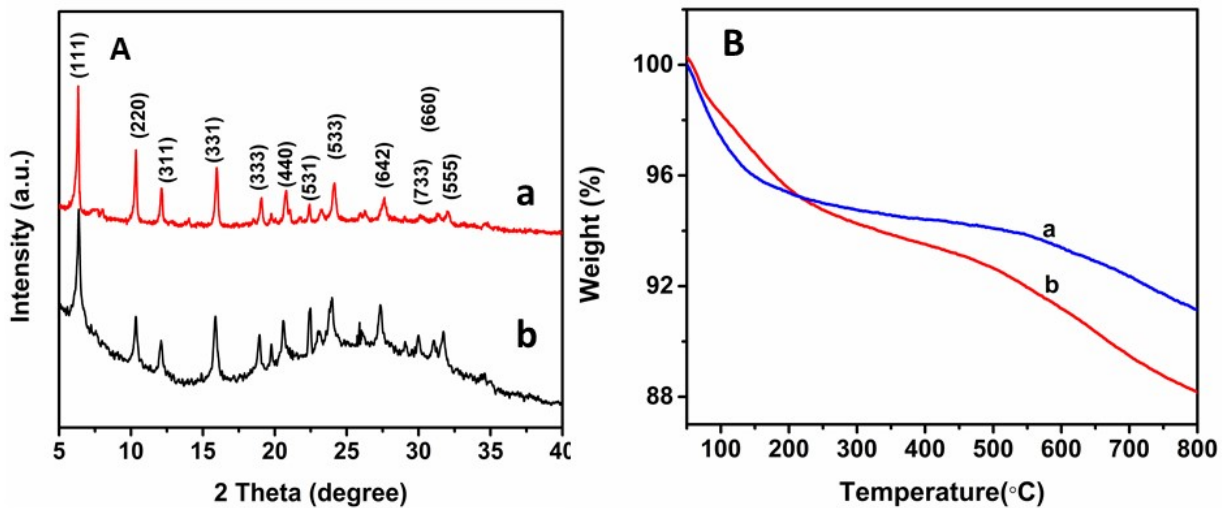


3

4 Fig. S10. Effect of a) Temperature, b) Duration, c) Mole ratio of methanol to TBA, and d)
5 different alcohols on MTBE synthesis using SAP-37MoC-4R.

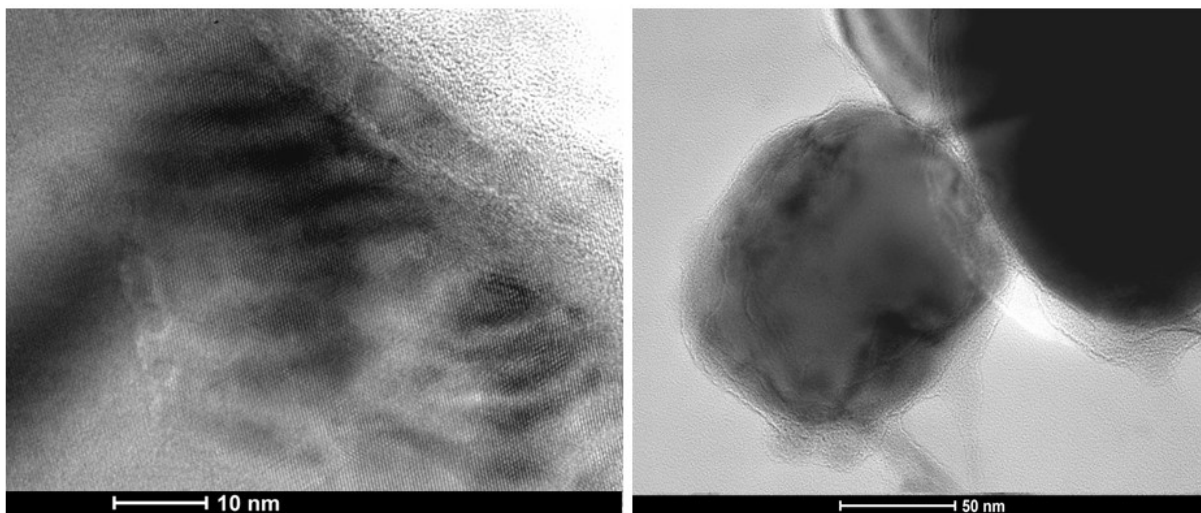
6

1



2

3 Fig. S11. Analysis of spent catalyst SAP-37MoC-4R A) powder XRD of a) SAP-37MoC-4R,
4 and b) spent catalyst; B) TGA profile of a) regenerated catalyst, and b) spent catalyst.



5

6 Fig. S12. TEM images of used SAP-37MoC-4R catalyst.

7

8

1 Table S6. MTBE synthesis using different catalysts.

Catalyst	Experimental condition	TBA conversion (%)	MTBE selectivity (%)
Mo-P/TiO ₂ ¹³	150 °C, 20 bar, LHSV= 1.0	78	75
W-P/TiO ₂ ¹³	150 °C, 20 bar, LHSV= 1.0	77	77
W-P/SiO ₂ ¹³	150 °C, 20 bar, LHSV= 1.0	81	89
W-P/Al ₂ O ₃ ¹³	150 °C, 20 bar, LHSV= 1.0	76	81
SAP-37MoC-4R	150 °C, 6 h, autogenous pressure	83	99

Catalyst	Experimental condition	isobutene conversion (%)	isobutene selectivity (%)
Amb-15 ^{RS1}	90 °C, 2 Mpa, WHSV=14 h ⁻¹	90	97
Zeolite beta ^{RS1}	90 °C, 2 Mpa, WHSV=14 h ⁻¹	82	90

2

3

4 References

5 **RS1.** F. Collignon, R. Loenders, J. A. Martens, P. A Jacobs and G. Poncelet, *J. Catal.*,
6 1999, **182**, 302.

7

8